Electronic Supplementary Material (ESI) for Journal of Materials Chemistry B.

SURFACTANT FREE LIQUID EXFOLIATED COPPER HYDROXIDE NANOCUBOIDS FOR NON-ENZYMATIC ELECTROCHEMICAL GLUCOSE DETECTION

Peter J. Lynch[1], Aline Amorim Graf[1], Sean P. Ogilvie[1], Matthew J. Large[1], Jonathan P. Salvage[2], Alan B. Dalton[1]

1 University of Sussex, Department of Physics and Astronomy, Brighton, BN1 9RH, UK

2 University of Brighton, School of Pharmacy and Biomolecular Science, Brighton, BN2 4GJ, UK

Sample	**R**	**G**	**B**
XL	76	146	155
L	46	143	157
M	29	119	120
S	20	101	107
XS	19	91	79
XXS	54	122	78

Table 1 RGB analysis of vacuum filtered $Cu(OH)_2$ films

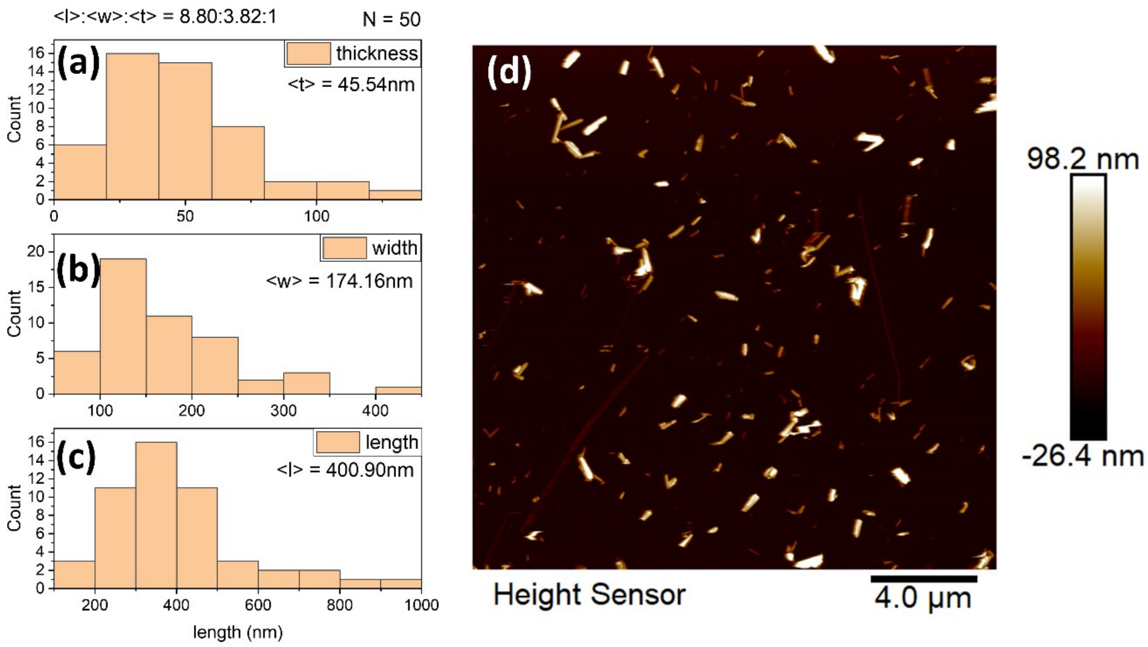

Figure 1 Statistics of L fraction of Cu(OH)2 flakes for (a) thickness, (b) width and (c) length. (d) a typical micrograph of the flakes

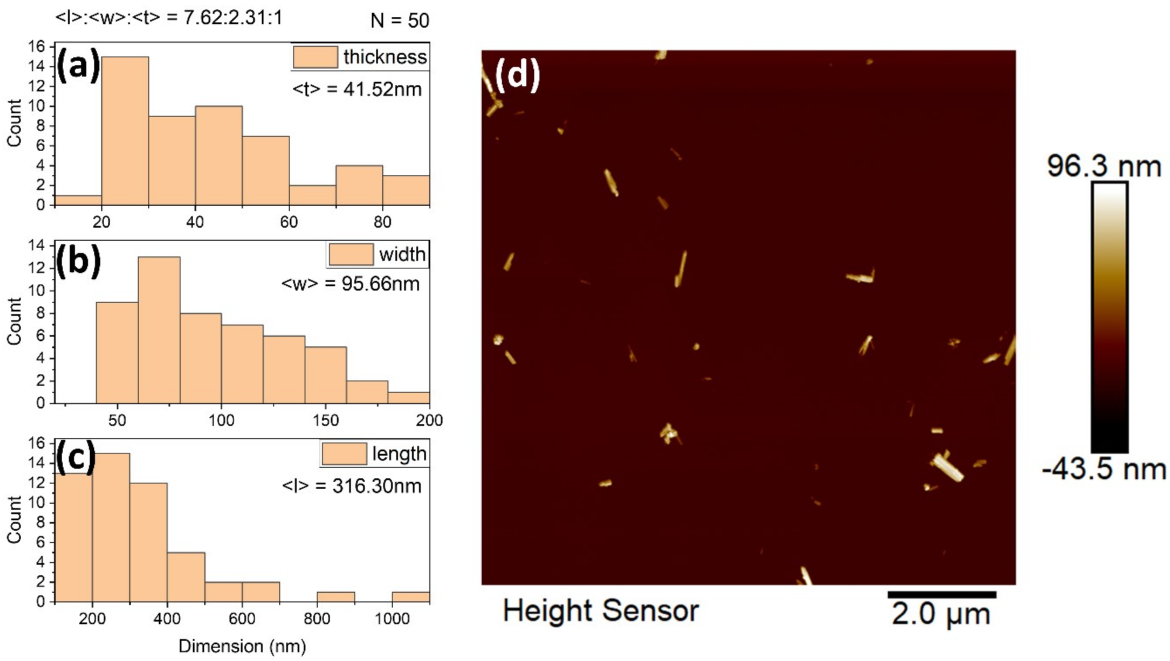

Figure 2 Statistics of M fraction of Cu(OH)2 flakes for (a) thickness, (b) width and (c) length. (d) a typical micrograph of the flakes

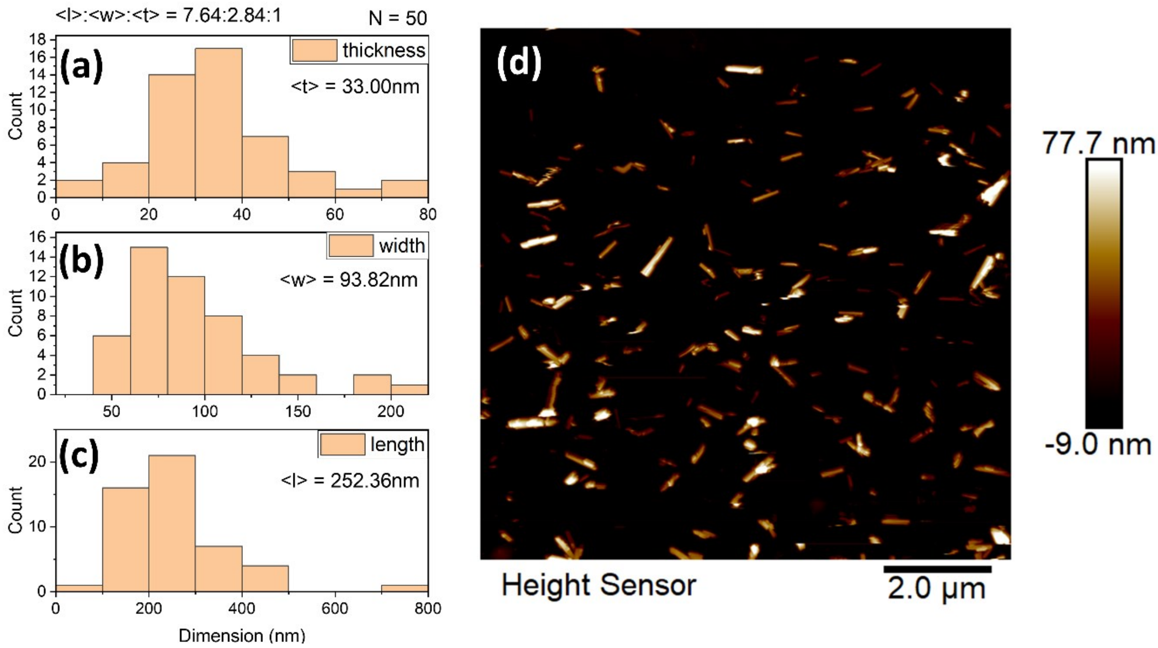

Figure 3 Statistics of S fraction of Cu(OH)2 flakes for (a) thickness, (b) width and (c) length. (d) a typical micrograph of the flakes

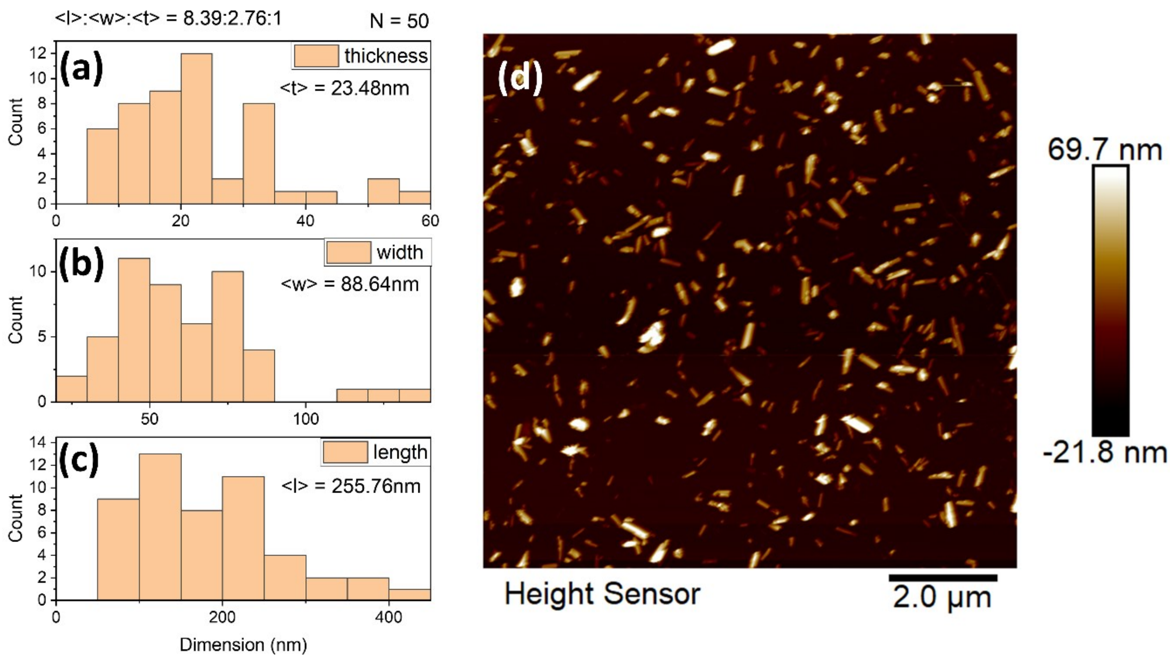

Figure 4 Statistics of XS fraction of Cu(OH)2 flakes for (a) thickness, (b) width and (c) length. (d) a typical micrograph of the flakes

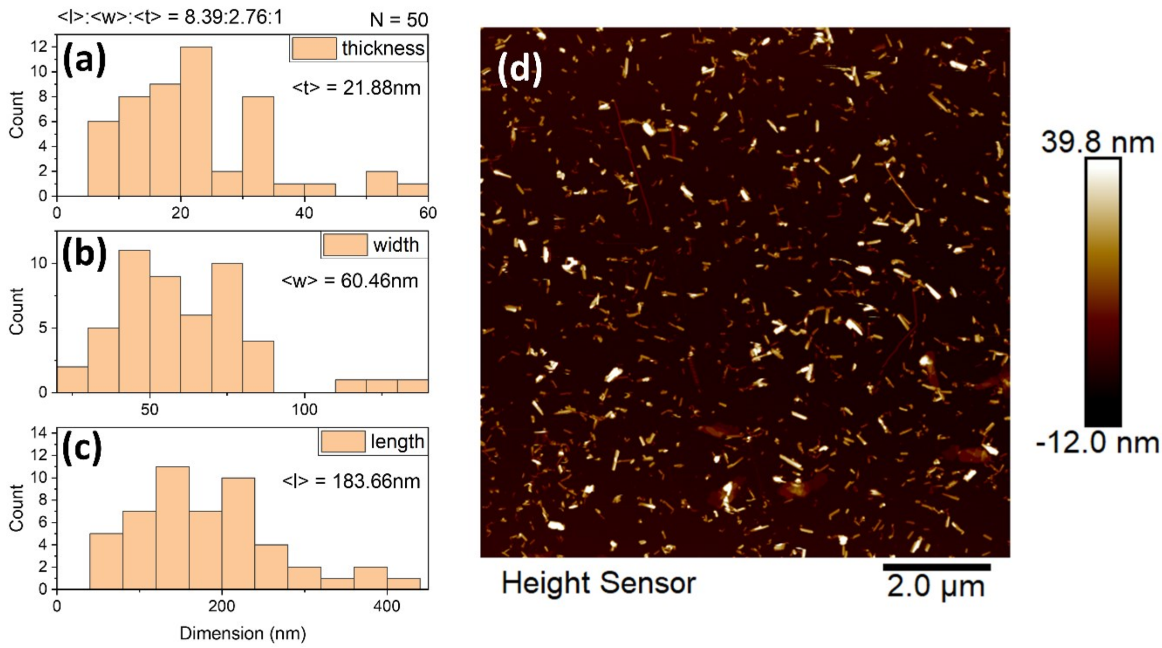

Figure 5 Statistics of XXS fraction of Cu(OH)2 flakes for (a) thickness, (b) width and (c) length. (d) a typical micrograph of the flakes

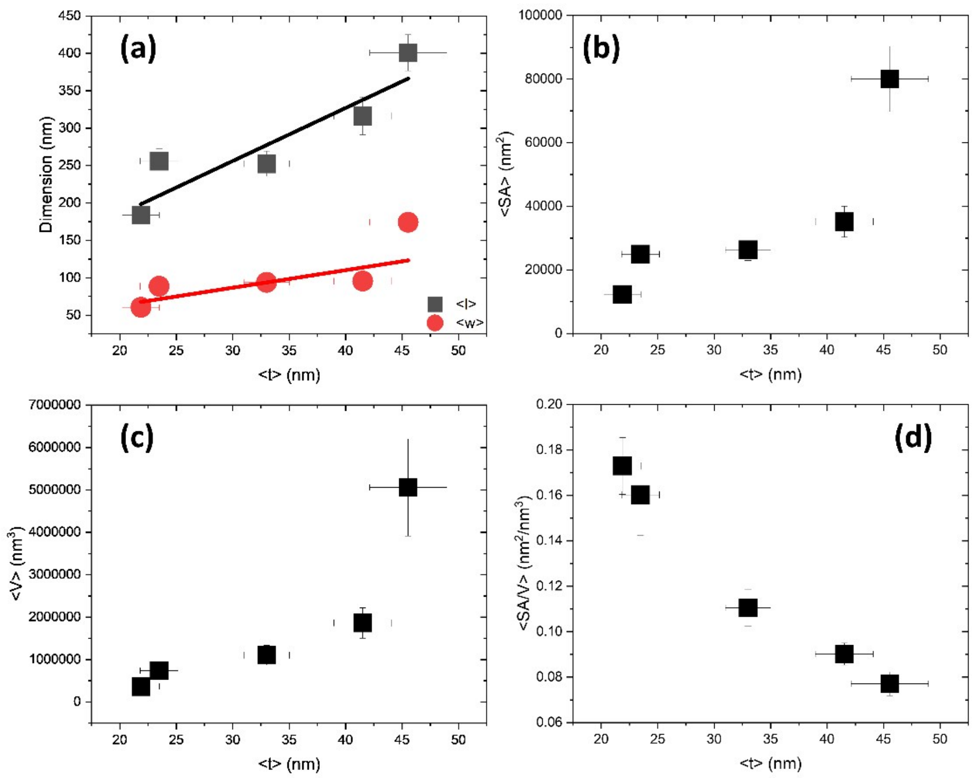

Figure 6 S7 (a) average length and width of size-selected $Cu(OH)_2$ nanocuboids plotted against thickness(b) average surface area plotted against thickness (c) average volume against thickness (d) average surface area to volume ratio plotted against thickness

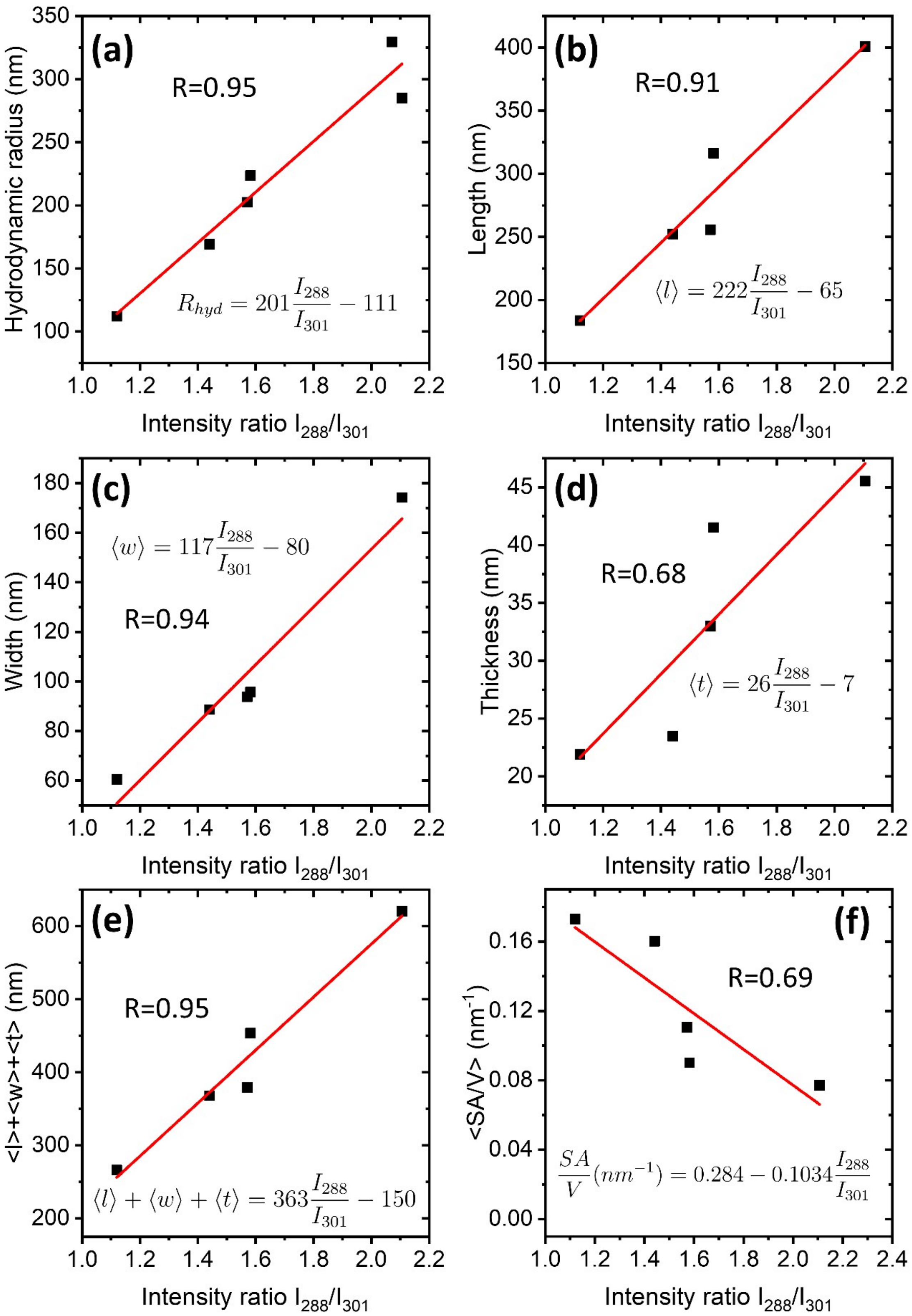

Figure 7 (a) Hydrodynamic Radius plotted against the intensity ratio of the 288 and 301 peaks (b-f) average length, width, thickness, sum of averages and average surface area per unit area plotted against peak intensity ratios

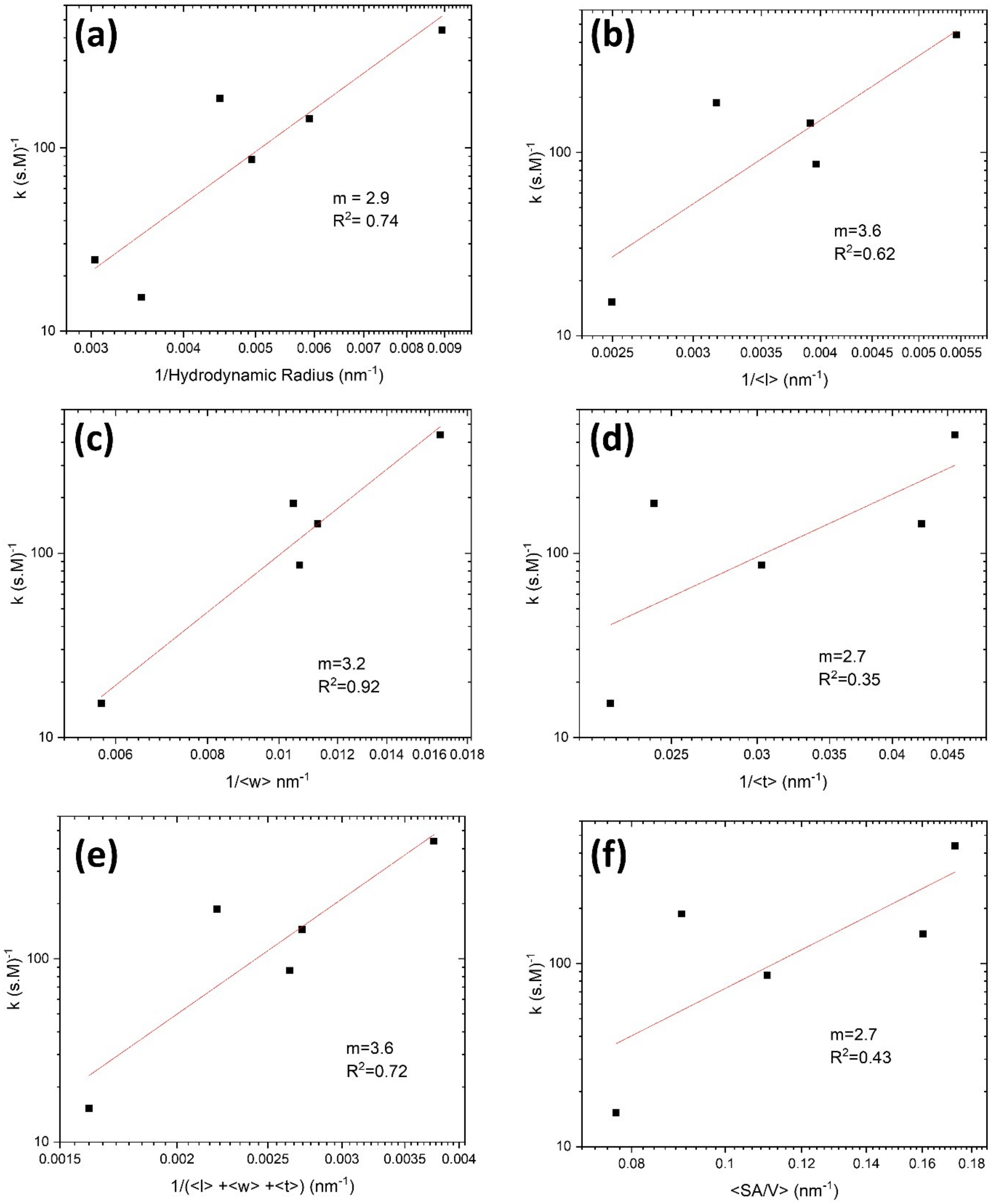

Figure 8 dependence of rate constant on average size dimensions as derived from AFM (a) 1/Hydrodynamic radium (b) 1/length (c) 1/width (d) 1/thickness (e)1/(average length + average width + average thickness) and (f) average surface area per unit volume

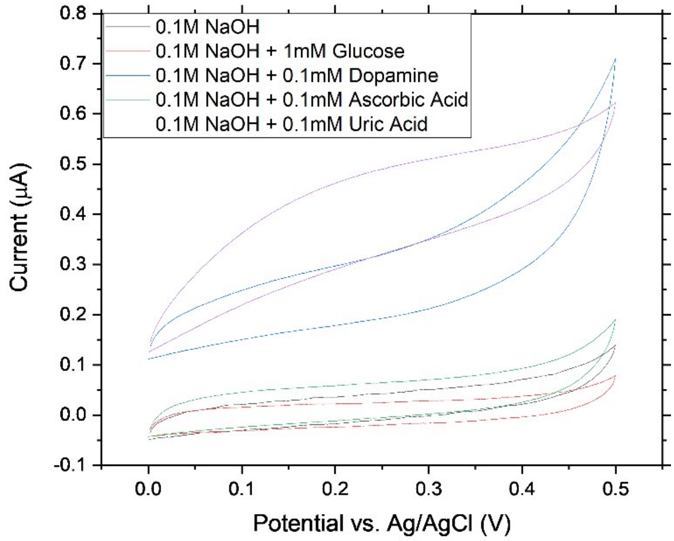

Figure 9 cyclic voltammograms of bare glassy carbon substrate in a variety of electrolytes

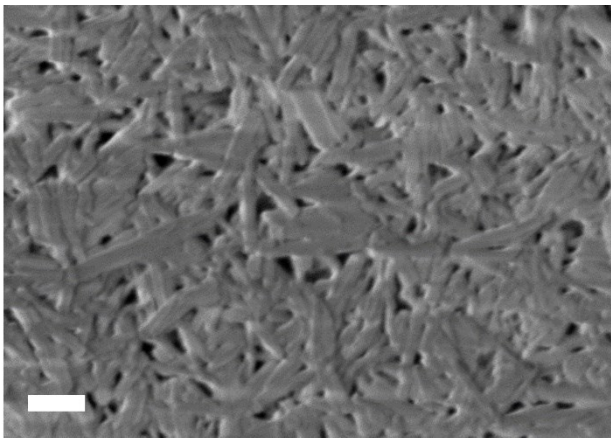

Figure 10 Sample SEM of XXS film (the scale bar, white, is 200nm)

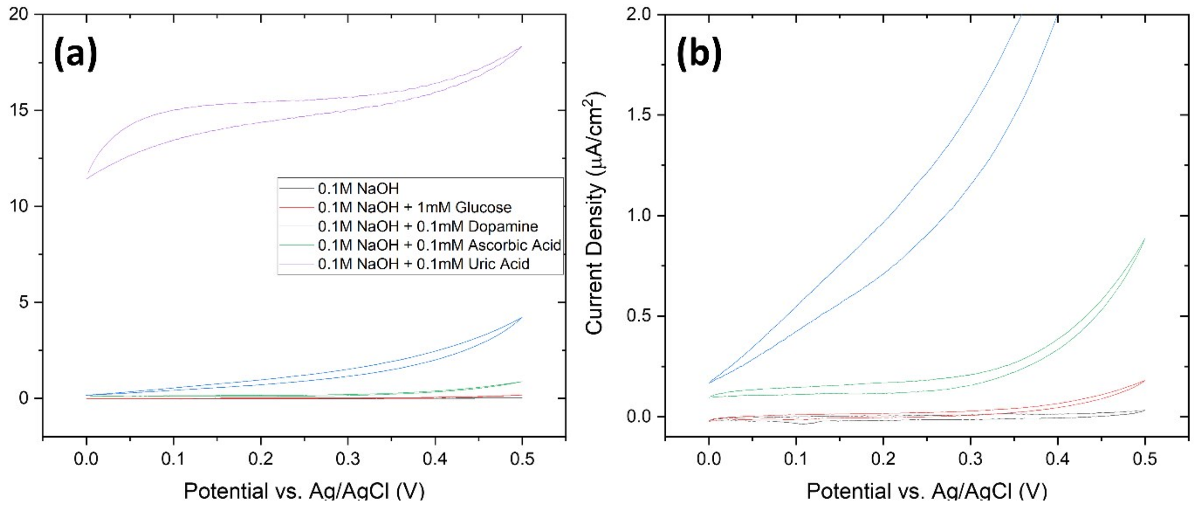

Figure 11 (a) cyclic voltammograms of bare ITO substrate in a variety of electrolytes (b) low current range

Figure 12 (a) cyclic voltammograms of bare ITO substrate in a variety of electrolytes (b) low current range

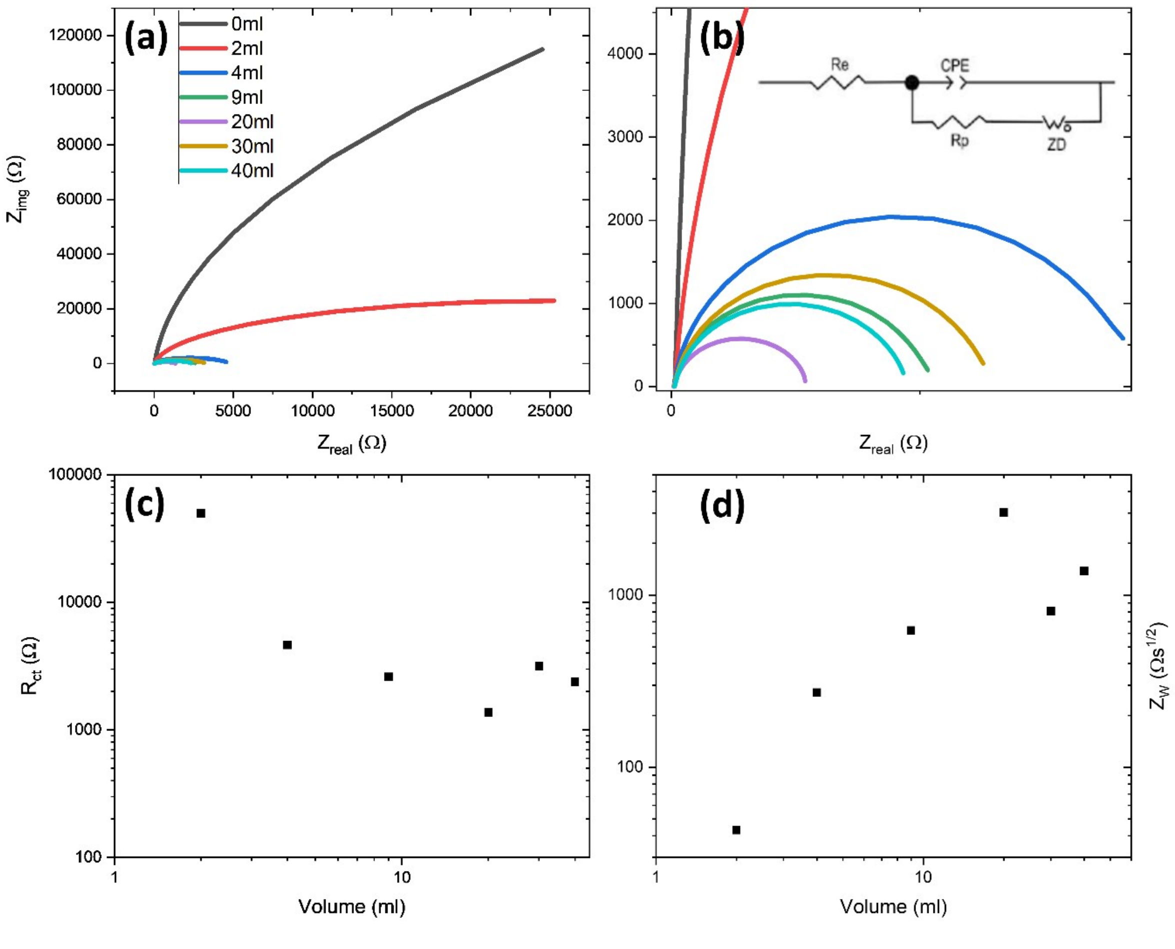

Figure 12 (a) Nyquist plot of different sprayed thicknesses of XXS fraction Cu(OH)2 taken at 0.5V vs. Ag/AgCl (b) low impedance region on same plot (inset) schematic of model used to fit plots (c) charge transfer resistance plotted against volume deposited (d) Warburg impedance plotted against volume deposited

Ref	Stoiciometery	Additives	Substrate	Sensitivity (mA/M.cm^2)	Linear range(mM)	LOD (µM)	Selectivity
1	HKUST-1	None	GCE	682-1044	0.002-4	0.6	DA,AA,UA,NaCl
2	Cu	MWCNT/Nafion	GCE	249	0-3.5	0.21	AA, UA, AAP
3	Cu	rGO	GCE	123	0-4	0.5	AA, DA, UA, and carbohydrates

4	Cu		FTO	1862	0-8	0.048	AA,UA, Lactose, Sucrose, Mannose, Fructose
5	Cu	Laser induced Graphene	Zinc Foil	495	0-6	0.39	AA,UA
6	Cu(CuNWs)	Nafion	GCE	420	0-2	0.035	UA,AA,sucrose,fructose,acetaminophen
7	Cu(OH)2	None	Porous graphene Foam	3360	0.0012-6	0.8	DA,AA,APAP,Fructose,Sucrose, Urea
8	CuO		Ta/Cu foil	2596	.0004-1.2	0.2	AA, UA, DA and carbohydrates
9	CuO		ITO	539	.0001-2	0.06	Comprehensive
10	CuO	Nafion	GCE	431	0.006-2.5	0.8	Fructose, Sucrose, Malt Dust
11	CuO		Cu Foil	2450	0.05-2	0.048	AA, UA and carbohydrates
12	CuS	MoS2	GCE	221	0.001-0.1	0.3	AA,UA, DA, sucrose

Table 2 copper based non-enzymatic glucose sensors

References

(1) Shahrokhian, S.; Khaki Sanati, E.; Hosseini, H. Direct Growth of Metal-Organic Frameworks Thin Film Arrays on Glassy Carbon Electrode Based on Rapid Conversion Step Mediated by Copper Clusters and Hydroxide Nanotubes for Fabrication of a High Performance Non-Enzymatic Glucose Sensing Platform. *Biosensors and Bioelectronics* **2018**, *112*, 100–107. https://doi.org/10.1016/j.bios.2018.04.039.

(2) Kang, X.; Mai, Z.; Zou, X.; Cai, P.; Mo, J. A Sensitive Nonenzymatic Glucose Sensor in Alkaline Media with a Copper Nanocluster/Multiwall Carbon Nanotube-Modified Glassy Carbon Electrode. *Analytical Biochemistry* **2007**, *363* (1), 143–150. https://doi.org/10.1016/j.ab.2007.01.003.

(3) Luo, J.; Jiang, S.; Zhang, H.; Jiang, J.; Liu, X. A Novel Non-Enzymatic Glucose Sensor Based on Cu Nanoparticle Modified Graphene Sheets Electrode. *Analytica Chimica Acta* **2012**, *709*, 47–53. https://doi.org/10.1016/j.aca.2011.10.025.

(4) Siampour, H.; Abbasian, S.; Moshaii, A. Copper Columnar Nanostructures Fabricated by Glancing Angle Deposition as a Robust and Scalable Method for High Sensitive Non-Enzymatic Glucose Detection. *Applied Surface Science* **2020**, *518*, 146182. https://doi.org/10.1016/j.apsusc.2020.146182.

(5) Zhang, Y.; Li, N.; Xiang, Y.; Wang, D.; Zhang, P.; Wang, Y.; Lu, S.; Xu, R.; Zhao, J. A Flexible Non-Enzymatic Glucose Sensor Based on Copper Nanoparticles Anchored on Laser-Induced Graphene. *Carbon* **2020**, *156*, 506–513. https://doi.org/10.1016/j.carbon.2019.10.006.

(6) Zhang, Y.; Su, L.; Manuzzi, D.; de los Monteros, H. V. E.; Jia, W.; Huo, D.; Hou, C.; Lei, Y. Ultrasensitive and Selective Non-Enzymatic Glucose Detection Using Copper Nanowires. *Biosensors and Bioelectronics* **2012**, *31* (1), 426–432. https://doi.org/10.1016/j.bios.2011.11.006.

(7) Shackery, I.; Patil, U.; Pezeshki, A.; Shinde, N. M.; Kang, S.; Im, S.; Jun, S. C. Copper Hydroxide Nanorods Decorated Porous Graphene Foam Electrodes for Non-Enzymatic Glucose Sensing. *Electrochimica Acta* **2016**, *191*, 954–961. https://doi.org/10.1016/j.electacta.2016.01.047.

(8) Jiang, L.-C.; Zhang, W.-D. A Highly Sensitive Nonenzymatic Glucose Sensor Based on CuO Nanoparticles-Modified Carbon Nanotube Electrode. *Biosensors and Bioelectronics* **2010**, *25* (6), 1402–1407. https://doi.org/10.1016/j.bios.2009.10.038.

(9) Li, Y.-Y.; Kang, P.; Huang, H.-Q.; Liu, Z.-G.; Li, G.; Guo, Z.; Huang, X.-J. Porous CuO Nanobelts Assembly Film for Nonenzymatic Electrochemical Determination of Glucose with High Fabrication Repeatability and Sensing Stability. *Sensors and Actuators B: Chemical* **2020**, *307*, 127639. https://doi.org/10.1016/j.snb.2019.127639.

(10) Wang, W.; Zhang, L.; Tong, S.; Li, X.; Song, W. Three-Dimensional Network Films of Electrospun Copper Oxide Nanofibers for Glucose Determination. *Biosensors and Bioelectronics* **2009**, *25* (4), 708–714. https://doi.org/10.1016/j.bios.2009.08.013.

(11) Zhuang, Z.; Su, X.; Yuan, H.; Sun, Q.; Xiao, D.; Choi, M. M. F. An Improved Sensitivity Non-Enzymatic Glucose Sensor Based on a CuO Nanowire Modified Cu Electrode. *Analyst* **2008**, *133* (1), 126–132. https://doi.org/10.1039/B712970J.

(12) Gao, Z.; Lin, Y.; He, Y.; Tang, D. Enzyme-Free Amperometric Glucose Sensor Using a Glassy Carbon Electrode Modified with Poly(Vinyl Butyral) Incorporating a Hybrid Nanostructure Composed of

Molybdenum Disulfide and Copper Sulfide. *Microchim Acta* **2017**, *184* (3), 807–814. https://doi.org/10.1007/s00604-016-2061-7.